

Oscillating Casimir potential between two impurities in a spin-orbit-coupled Bose-Einstein condensate

 Pei-Song He,¹ Qing Sun,^{2,*} and An-Chun Ji²
¹*School of Science, Beijing Technology and Business University, Beijing 100048, China*
²*Department of Physics, Capital Normal University, Beijing 100048, China*

(Received 4 September 2017; published 18 October 2017)

We study the Casimir potential between two impurities immersed in a spin-orbit-coupled Bose-Einstein condensate (BEC) with plane-wave order. We find that by exchanging the virtual excitations, a remarkable anisotropic oscillating potential with both positive and negative parts can be induced between the impurities, with the period of the oscillation depending on the spin-orbit-coupling strength. As a consequence, this would inevitably lead to a noncentral Casimir force, which can be tuned by varying the strength of the spin-orbit coupling (SOC). These results are elucidated for BECs with one-dimensional Raman-induced and two-dimensional Rashba-type SOC.

 DOI: [10.1103/PhysRevA.96.043617](https://doi.org/10.1103/PhysRevA.96.043617)

I. INTRODUCTION

Research on the quantum impurity problem in a many-body system provides a promising way to study the few-body and many-body physics in condensed matter physics [1–10]. The interplay between the impurity and the background many-body ground state can lead to many intriguing phenomena [11–21], such as the orthogonality catastrophe of a time-dependent impurity in ultracold fermions [22,23], an electron dressing Bose-Einstein condensate (BEC) by a Rydberg-type impurity [24], and the Yu-Shiba-Rusinov state [25–29]. One of the remarkable effect is that an effective interaction may be induced between impurities via exchanging the virtual excitations of the underlying ground-state fluctuations, which is also known as the Casimir effect [30–36].

In recent years, with the realization of artificial gauge fields in ultracold atoms, the spin-orbit-coupled quantum gases have attracted attentive studies and many interesting physics brought by spin-orbit coupling (SOC) have been explored [37,38]. For example, a plane-wave (PW) phase and a stripe phase can be identified in BECs with SOC [39]. More recently, it was found that a point-like impurity moving in a Bose-Einstein condensate with a Rashba SOC would experience a drag force with a nonzero transverse component [40], and a Fulde-Ferrell-Larkin-Ovchinnikov-like molecular state [41,42] may exist in spin-orbit-coupled Fermi gas. Based on these developments of SOC and impurity physics in ultracold atoms, a natural and important question is then raised: How is the Casimir potential between impurities in a BEC affected by SOC?

To address this problem, in this paper we calculate the instantaneous Casimir potential between two impurities immersed in a BEC with SOC. We find that by exchanging the virtual excitations of the PW phase, the inter-impurity potential exhibits a remarkable oscillating behavior with both repulsive and attractive components. Specifically, for the Raman-induced one-dimensional (1D) SOC, such oscillation only exists along the direction of the SOC. While for the two-dimensional (2D) Rashba SOC, the potential oscillates in

both directions with different oscillation periods: The period in the direction of the PW wave vector is about half of the one along the perpendicular direction. Such anisotropy of the potential would inevitably lead to a noncentral Casimir force between the impurities.

This paper is organized as follows: First in Sec. II, we model the system and present the general formalism. Then, we analyze the results and underlying physics in Sec. III. Finally in Sec. IV, we give a brief summary.

II. MODEL AND FORMALISM

A. Model

We consider two impurity atoms immersed in a two-component interacting Bose gas with SOC. The Hamiltonian of the system can be written as

$$\begin{aligned}
 H = \int d\mathbf{r} \hat{\phi}^\dagger(\mathbf{r}) & \left[-\frac{\hbar^2 \nabla^2}{2m_B} - \mu - i \sum_{i,j=x,y,z} v_{ij} \partial_i \sigma_j \right. \\
 & \left. + \sum_{i=x,y,z} \Lambda_i \sigma_i \right] \hat{\phi}(\mathbf{r}) + \frac{1}{2} \int d\mathbf{r} [g_{\uparrow\uparrow} \hat{n}_\uparrow^2 + 2g_{\uparrow\downarrow} \hat{n}_\uparrow \hat{n}_\downarrow \\
 & + g_{\downarrow\downarrow} \hat{n}_\downarrow^2] + \int d\mathbf{r} \hat{\psi}^\dagger(\mathbf{r}) \left(-\frac{\hbar^2 \nabla^2}{2m_I} \right) \hat{\psi}(\mathbf{r}) \\
 & + g_I \int d\mathbf{r} \hat{n}(\mathbf{r}) \hat{\psi}^\dagger(\mathbf{r}) \hat{\psi}(\mathbf{r}). \quad (1)
 \end{aligned}$$

Here, $\hat{\phi}(\mathbf{r}) = (\hat{\phi}_\uparrow(\mathbf{r}), \hat{\phi}_\downarrow(\mathbf{r}))^T$ and $\hat{\psi}(\mathbf{r})$ are the annihilation operators of the two-component boson and impurity atom fields (boson or fermion) at position \mathbf{r} , with the mass m_B and m_I , respectively. $\hat{n} = \hat{n}_\uparrow + \hat{n}_\downarrow$ denotes the density operator with $\hat{n}_\uparrow = \hat{\phi}_\uparrow^\dagger \hat{\phi}_\uparrow$ and $\hat{n}_\downarrow = \hat{\phi}_\downarrow^\dagger \hat{\phi}_\downarrow$. σ_x , σ_y and σ_z are the Pauli matrices. μ is the chemical potential of bosons. v_{ij} and Λ_i ($i, j = x, y, z$) describe the strength of effective SOC and magnetic field along the i direction. $g_{\uparrow\uparrow}$ ($= g_{\downarrow\downarrow}$) and $g_{\uparrow\downarrow}$ are the intra- and intercomponent interactions between bosons, while the impurity atoms couple to the bosons via a density-density interaction with strength g_I . In this paper, we are interested in the unique features of the induced interaction

*sunqing@cnu.edu.cn

between impurities introduced by the SOC, which is shown to be independent with the statistics of the impurity atom. Further for simplicity, we have neglected the possible direct interaction between impurity atoms, which would not affect the main physics essentially.

B. Casimir potential between two impurities

Before proceeding, let us briefly discuss the effects brought about by SOC. It is well known that in the absence of impurities, the presence of SOC would largely change the single-particle spectrum, and give rise to degenerate single-particle ground states, e.g. double minima for Raman-induced 1D SOC and ring degeneracy for Rashba SOC. Here, the 1D SOC (along the x direction) corresponds to $v_{xz} = -\hbar^2 k_L/m_B$, $\Lambda_x = \Omega$ and the Rashba SOC has $v_{xx} = v_{yy} = \hbar^2 k_L/m_B$ with k_L and Ω the strengths of SOC and Raman coupling, respectively. In both cases, all of the other v_{ij} and Λ_i ($i, j = x, y, z$) are zero. As a result, the many-body ground state for a homogeneous Bose-Einstein condensate could be in a PW phase or a stripe phase, depending on the atomic interaction parameter $\eta = g_{\uparrow\downarrow}/g_{\uparrow\uparrow}$ [39,43,44]. Correspondingly, the excitation spectrum of each phase would be also changed dramatically. When the impurities get involved, they would interplay with such excitations of the background condensate, and a unique SOC-dependent interaction may be induced between the impurities. To show this more concretely, we take the PW ground state as an example in the following.

In the path-integral formalism, we write the partition function of Hamiltonian (1) as $\mathcal{Z} = \int \mathcal{D}[\bar{\phi}, \phi, \bar{\psi}, \psi] e^{-\frac{1}{\hbar} S[\bar{\phi}, \phi, \bar{\psi}, \psi]}$, with $S[\bar{\phi}, \phi, \bar{\psi}, \psi] = \int_0^\beta d\tau [\hbar \bar{\phi} \partial_\tau \phi + \hbar \bar{\psi} \partial_\tau \psi + H(\bar{\phi}, \phi, \bar{\psi}, \psi)]$. For a low average density of the impurity atoms and moderate impurity-boson interactions, it is assumed that we can safely neglect the modifications on the properties of the condensate as well as the dispersion of the excitations due to the impurities [30]. In this way, we further write the boson fields as $\phi(\mathbf{r}, \tau) = \phi_0(\mathbf{r}) + \delta\phi(\mathbf{r}, \tau)$, where $\phi_0(\mathbf{r})$ is the wave function of the condensate and $\delta\phi(\mathbf{r}, \tau)$ are quantum fluctuations above the condensate. In the PW phase, we have $\phi_0(\mathbf{r}) = \sqrt{n_0}(u, v)^T e^{i\mathbf{k}_0 \cdot \mathbf{r}}$ with \mathbf{k}_0 the condensed momentum of the plane wave. n_0 is the density of the condensed bosons and u and v are the relative amplitudes of each component satisfying $|u|^2 + |v|^2 = 1$.

To facilitate the following discussions, we turn to the momentum-frequency space via the Fourier transformation

$$\delta\phi(\mathbf{r}, \tau) = (\hbar\beta V)^{-1/2} e^{i\mathbf{k}_0 \cdot \mathbf{r}} \sum_{\mathbf{q}, \nu} \delta\phi(\mathbf{q}, \nu) e^{i\mathbf{q} \cdot \mathbf{r} - i\nu\tau}, \quad (2)$$

$$\psi(\mathbf{r}, \tau) = (\hbar\beta V)^{-1/2} \sum_{\mathbf{k}, \omega} \psi(\mathbf{k}, \omega) e^{i\mathbf{k} \cdot \mathbf{r} - i\omega\tau}. \quad (3)$$

Here, \mathbf{q} (relative to the condensed momentum \mathbf{k}_0) and \mathbf{k} are the momenta of the quantum fluctuation $\delta\phi(\mathbf{q}, \nu)$ and the impurity field $\psi(\mathbf{k}, \omega)$, respectively. ν and ω are Matsubara frequencies in the imaginary time.

Within the Bogoliubov approximation of a weakly interacting gas, the partition function can be expanded up to second order, which becomes $\mathcal{Z} = \int \mathcal{D}[\delta\bar{\phi}, \delta\phi, \delta\bar{\psi}, \delta\psi] e^{-\frac{1}{\hbar} [S_0 + S^{(2)}]}$. Here, S_0 is the action in the classical level, and $S^{(2)}$ is the

Gaussian part, which is given by

$$\begin{aligned} S^{(2)} &= \frac{1}{2} \sum_{\mathbf{q}, \nu} \delta\bar{\Phi}(\mathbf{q}, \nu) \mathbf{M}(\mathbf{q}, \nu) \delta\Phi(\mathbf{q}, \nu) \\ &+ \sum_{\mathbf{k}, \omega} \frac{\hbar^2 \mathbf{k}^2}{2m_I} \bar{\psi}(\mathbf{k}, \omega) \psi(\mathbf{k}, \omega) \\ &+ \frac{1}{2} \sum_{\mathbf{q}, \nu} [\mathbf{J}^\dagger(\mathbf{q}, \nu) \delta\Phi(\mathbf{q}, \nu) + \text{H.c.}], \end{aligned} \quad (4)$$

where $\delta\Phi(\mathbf{q}, \nu) = [\delta\phi_\uparrow(\mathbf{q}, \nu), \delta\phi_\downarrow(\mathbf{q}, \nu), \delta\bar{\phi}_\uparrow(-\mathbf{q}, -\nu), \delta\bar{\phi}_\downarrow(-\mathbf{q}, -\nu)]^T$, $\mathbf{J}(\mathbf{q}, \nu) = g_I \sqrt{n_0} \rho(\mathbf{q}, \nu)(u, v, u, v)^T$ with $\rho(\mathbf{q}, \nu) = \sum_{\mathbf{k}, \omega} \bar{\psi}(\mathbf{k}, \omega) \psi(\mathbf{k} + \mathbf{q}, \omega + \nu)$, and

$$\mathbf{M}(\mathbf{q}, \nu) = -i\hbar\nu \begin{pmatrix} I & 0 \\ 0 & -I \end{pmatrix} + \begin{pmatrix} A_{\mathbf{q}} + B & B \\ B & A_{-\mathbf{q}}^\dagger + B \end{pmatrix} \quad (5)$$

with I the 2×2 unit matrix and

$$\begin{aligned} A_{\mathbf{q}} &= H_0(\mathbf{q} + \mathbf{k}_0)I - \mu I + \eta g n_0 I - (\eta - 1) g n_0 \begin{bmatrix} u^2 & 0 \\ 0 & v^2 \end{bmatrix}, \\ B &= g n_0 \begin{bmatrix} u^2 & \eta uv \\ \eta uv & v^2 \end{bmatrix}. \end{aligned} \quad (6)$$

Here, $H_0(\mathbf{q}) = \frac{\hbar^2 \mathbf{q}^2}{2m_B} + \sum_{i,j=x,y,z} v_{ij} q_i \sigma_j + \sum_{i=x,y,z} \Lambda_i \sigma_i$.

We further introduce the time-ordered Green's function of the boson fields $\delta\Phi$ as

$$\mathcal{G}_0(\mathbf{r}, \tau; \mathbf{r}', \tau') \equiv -\frac{1}{2\hbar} \langle 0 | T_\tau \delta\Phi(\mathbf{r}, \tau) \delta\bar{\Phi}(\mathbf{r}', \tau') | 0 \rangle, \quad (7)$$

and its Fourier transformation

$$\begin{aligned} \mathcal{G}_0(\mathbf{r}, \tau; \mathbf{r}', \tau') &= \frac{1}{\hbar\beta V} \sum_{\mathbf{q}, \nu} \mathcal{G}_0(\mathbf{q}, \nu) e^{i\mathbf{q} \cdot (\mathbf{r} - \mathbf{r}') - i\nu(\tau - \tau')}, \\ \mathcal{G}_0(\mathbf{q}, \nu) &= [-\mathbf{M}(\mathbf{q}, \nu)]^{-1}. \end{aligned} \quad (8)$$

Here, $|0\rangle$ is the vacuum state in the quasiparticle basis. Then the effective action for impurities can be obtained by integrating out the fluctuations of boson fields in Eq. (4), which gives

$$\begin{aligned} S_{\text{eff}} &= \int_0^{\hbar\beta} d\tau \int d\mathbf{r} \bar{\psi}(\mathbf{r}, \tau) \left(\hbar \partial_\tau - \frac{\hbar^2 \nabla^2}{2m_I} \right) \psi(\mathbf{r}, \tau) \\ &+ \frac{1}{2} \int_0^{\hbar\beta} d\tau d\tau' \int d\mathbf{r} d\mathbf{r}' \\ &\times |\psi(\mathbf{r}, \tau)|^2 V(\mathbf{r}, \tau; \mathbf{r}', \tau') |\psi(\mathbf{r}', \tau')|^2, \end{aligned} \quad (9)$$

where

$$\begin{aligned} V(\mathbf{r}, \tau; \mathbf{r}', \tau') &= \frac{1}{\hbar\beta V} \sum_{\mathbf{q}, \nu} V(\mathbf{q}, \nu) e^{i\mathbf{q} \cdot (\mathbf{r} - \mathbf{r}') - i\nu(\tau - \tau')}, \\ V(\mathbf{q}, \nu) &= g_I^2 n_0 (u, v, u, v) \mathcal{G}_0(\mathbf{q}, \nu) (u, v, u, v)^T. \end{aligned} \quad (10)$$

Above, Eq. (10) is the main starting point of this paper. In general, the fluctuations of the condensate can mediate an interaction between impurities. And we are interested in the instantaneous component of $\nu = 0$ [30], which is justified by the dominant processes of emitting and absorbing of virtual quasiparticles between two impurities. In this case, the Casimir potential takes the form of $V(\mathbf{r}, \tau; \mathbf{r}', \tau') \simeq V(|\mathbf{r} - \mathbf{r}'|) \delta(\tau - \tau')$.

τ'), reflecting the “vacuum” energy modification from these exchanging of quasiparticles.

To explore the main features of the induced potential, in the following we take the Raman-induced 1D and Rashba-type SOCs as examples to demonstrate the underlying physics.

III. RESULTS

A. Raman-induced 1D SOC

In this case, the PW phase survives in the parameter regime with $0 < \alpha < 1$ ($\alpha \equiv \Omega m_B / \hbar^2 k_L^2$) and $\eta > \eta_c = (2 - 3\alpha^2)/(2 - \alpha^2)$, which would transit to a zero-momentum phase at $\alpha = 1$ [43]. For $\alpha \ll 1$, we have

$$\begin{aligned} u &= -\sin \frac{\gamma k_0}{2}, \\ v &= \cos \frac{\gamma k_0}{2}, \\ \mathbf{k}_0 &= -\sqrt{1 - \alpha^2} k_L \mathbf{e}_x, \end{aligned} \quad (11)$$

with $\sin \gamma k_0 = \Omega / \sqrt{(k_L k_0 / m_B)^2 + \Omega^2}$. Correspondingly, the chemical potential μ is given by

$$\begin{aligned} \mu &= \varepsilon_{\mathbf{k}_0 - \mathbf{k}_L} \sin^2 \frac{\gamma k_0}{2} + \varepsilon_{\mathbf{k}_0 + \mathbf{k}_L} \cos^2 \frac{\gamma k_0}{2} - \Omega \sin \gamma k_0 \\ &+ g n_0 + \frac{1}{2} (\eta - 1) g n_0 \sin^2 \gamma k_0 - \varepsilon_L, \end{aligned} \quad (12)$$

with $\varepsilon_L \equiv \hbar^2 k_L^2 / 2m_B$. With Eqs. (11) and (12), one can derive the explicit expression of the instantaneous Casimir potential $V(\mathbf{r})$ given by Eq. (10) (not shown here). In Fig. 1(a), we plot $V(\mathbf{r})$ in the plane of the relative coordinate \mathbf{r} with $\gamma = 3$. Here, $\gamma \equiv \xi^{-2} / k_L^2$ denotes the ratio between boson-boson interaction energy and the kinetic energy characterized by the strength of SOC, where $\xi = \hbar / \sqrt{2gn_0 m_B}$ is the healing length of the boson system. We find that, in contrast to that without SOC, the instantaneous Casimir potential exhibits a remarkable oscillation between repulsive and attractive parts with the varying of the distance between impurities. Furthermore, such oscillation is found to be along the x direction, with period about $\pi/|\mathbf{k}_0|$, as shown in Fig. 1(b).

The oscillating behavior can be understood as follows. In the basis of single-particle states of the free boson gas, the inter-impurity Casimir potential is a consequence of the

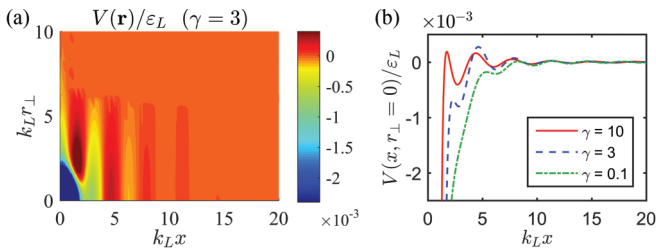


FIG. 1. (a) Distribution of the Casimir potential $V(\mathbf{r})$ (in units of ε_L) in the x, r_\perp plane of the relative coordinate \mathbf{r} between two impurities in a 3D BEC with Raman-induced 1D (along the x direction) SOC. (b) The Casimir potential $V(x, r_\perp = 0)$ along the x axis for $\gamma = 10, 3$, and 0.1 . Other parameters are $\alpha = 0.25$ and $\eta = 1.0$.

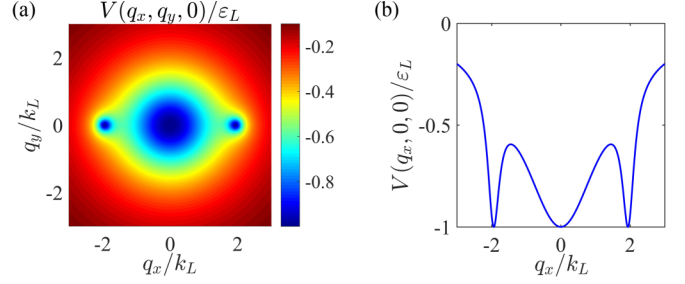


FIG. 2. Fourier distribution $V(\mathbf{q})$ of the Casimir potential $V(\mathbf{r})$ given in Fig. 1. (a) $V(q_x, q_y, 0)$ in the q_x, q_y plane with $q_z = 0$; (b) $V(q_x, 0, 0)$ along the q_x axis with $q_y = q_z = 0$. Here, $\alpha = 0.25$, $\eta = 1$, and $\gamma = 3$.

scattering between the condensed bosons and the excited ones, as can be seen in the last term of Eq. (4). In the static limit of impurity potential (that is, $v = 0$), it prefers the scattering process between states with small energy difference. To see it more clearer, in Fig. 2, we give the Fourier component $V(\mathbf{q})$ of the Casimir potential. One can see that for the Raman-induced 1D SOC, $V(\mathbf{q})$ is dominated by the excited states around the condensed momentum and those around the other degenerate momentum, with the exchanged momenta about zero and $\pm 2\mathbf{k}_0$, respectively. The distribution of $V(\mathbf{q})$ around zero momentum is common to that of the BEC without SOC, and it will contribute to an attractive, divergent, and damping Casimir potential. While that around $\pm 2\mathbf{k}_0$ is the unique feature brought by the Raman-induced 1D SOC, which gives rise to the oscillations of the potential with a period of about $\pi/|\mathbf{k}_0|$. It is noteworthy that this oscillating behavior bears some similarity to the well-known Ruderman-Kittel-Kasuya-Yosida (RKKY) indirect exchange between two localized spins. The main difference is that, the RKKY interaction is mediated by the delocalized fermions around the Fermi surface [45]. While in our case, the induced interaction is mediated by the bosonic excitations around the ground state with finite momentum. Moreover, due to the macroscopic occupancy of the condensed state, there is a bosonic enhancement n_0 in the Casimir potential, making the oscillations prominent.

We also find that the range of the Casimir potential is on the order of the healing length ξ , similar to that without SOC. Since the period of oscillation is about $\pi/|\mathbf{k}_0|$, the number of oscillations decreases for smaller $|\mathbf{k}_0|$, which can be achieved by making k_L smaller or α larger. Furthermore, as ξ gets larger, that is, for larger γ , the positive humps at small relative distance gradually become negative humps and even vanish, as shown in Fig. 1(b).

The amplitude of the oscillations grows quickly as the strength of SOC gets larger, as shown in Fig. 1 in which the Casimir potential is scaled with ε_L . So the Casimir potential can be prominent for large enough SOC strength. We have also calculated the Casimir potential in 2D with Raman-induced 1D SOC. By comparing the results in 2D and 3D systems, we find that the amplitude of the oscillation in the Casimir potential is more prominent in lower dimensional systems, which is because that the ratio of the those scatterings contribute to the oscillations to all of the scatterings is larger in lower

dimension. We also find that as η increases, the amplitude of the oscillations becomes diminished. This is because the gap of excitations which corresponds to momentum transfer around $\pm 2\mathbf{k}_0$ along the k_x axis becomes larger when η is increased, and it results in smaller scattering probability with corresponding transferred momentum.

Another important feature of the Casimir potential is that it is anisotropic due to the anisotropic excitation spectrum, which means that the Casimir force between the two impurities is noncentral. Similar behavior has also been found previously in drag force experienced by a moving impurity in BEC with SOC [40].

B. Rashba-type SOC

For isotropic Rashba SOC [44], the PW phase appears for $\eta \leq 1$. We have

$$\begin{aligned} u &= v = \frac{1}{\sqrt{2}}, \\ \mathbf{k}_0 &= -k_L \mathbf{e}_x, \end{aligned} \quad (13)$$

and

$$\mu = -\frac{\hbar^2 k_0^2}{2m_B} + gn_0 + 2(\eta - 1)gn_0 u^2 v^2. \quad (14)$$

After some straightforward calculations, the dimensionless Casimir potential takes

$$V(\mathbf{r}) = \int \frac{d^2 \mathbf{q}}{(2\pi)^2} V(\mathbf{q}) \cos(\mathbf{q} \cdot \mathbf{r}), \quad (15)$$

where

$$\begin{aligned} V(\mathbf{q}) &= -\frac{2g_I^2}{g} \gamma \{q^6 - 4q^2(2q_x^2 - q_y^2) + 16q_x^2 \\ &\quad + (1 - \eta)\gamma(q^4 + 4q_x^2)\} / \{(q^4 - 4q_x^2)^2 \\ &\quad + 2\gamma[q_x^2(q^2 - 4)^2 + q^2 q_y^2(q^2 + 4)] \\ &\quad + (1 - \eta^2)\gamma^2(q^4 + 4q_x^2) \\ &\quad - 4(1 - \eta)\gamma[q^4 + 4q_x^2(1 - q^2)]\}. \end{aligned} \quad (16)$$

It is interesting to see that in Eq. (16) $V(\mathbf{q})$ is just the dynamical structure factor at zero Matsubara frequency [46,47].

In Fig. 3, we plot the distributions of $V(\mathbf{r})$ and $V(\mathbf{q})$ in the real space and momentum space respectively. One can see that the potential in this situation also shows significant oscillating behavior as in the case of Raman-induced 1D SOC. Nevertheless, there are some important differences arising from the ring degeneracy of the single-particle states brought by the isotropic Rashba SOC.

First, the Casimir potential for the Rashba SOC oscillates along both x and y directions as depicted in Figs. 3(c) and 3(d). In particular, the periods of oscillation along both directions are found to be around π/k_L and $2\pi/k_L$, respectively. The reason is that due to the Rashba SOC, the scattering processes with momentum transfer around $2k_L$ and k_L along x and y directions between the impurity and the background BEC are largely enhanced. Second, along the y axis, a positive hump is developed [see Fig. 3(d)]. Third, with the decrease of η , the excitation gap along the x direction increases. As a

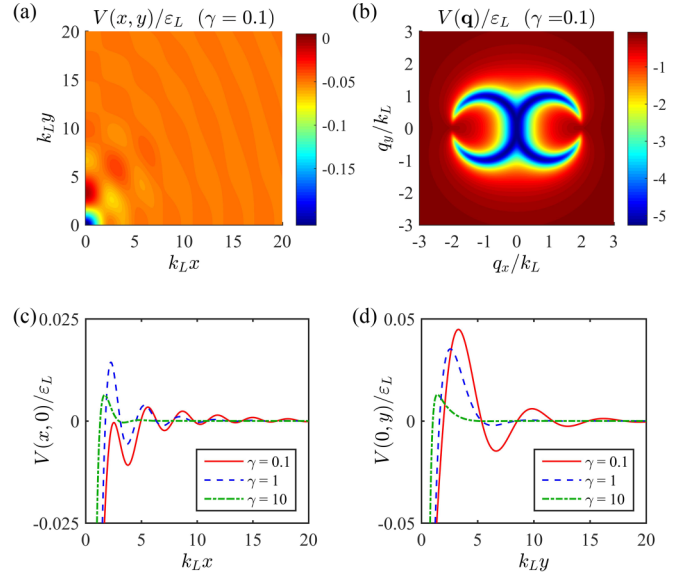


FIG. 3. (a) Real space distribution $V(x,y)$ and (b) momentum space distribution $V(q_x, q_y)$ of the Casimir potential between two impurities in a 2D BEC with Rashba-type SOC. (c) and (d) are the Casimir potentials along the x and y axes, respectively, with $\gamma = 0.1, 1, \text{ and } 10$. $\eta = g_{\uparrow\downarrow}/g = 0.9$.

result, the oscillating behavior along the x direction gradually diminishes. While the behavior of the potential along the y direction is not changed.

IV. CONCLUSIONS AND DISCUSSIONS

In conclusion, we have calculated the instantaneous Casimir potential between two impurities immersed in BECs with Raman-induced 1D SOC and Rashba-type SOC. We find that due to the SOC, the Casimir potential between impurities exhibits remarkable oscillations with both positive and negative components, and the period of the oscillation is inversely proportional to the strength of SOC. In addition, the amplitudes of the oscillations become prominent with increasing SOC strength, and can be further tuned by varying the atomic interactions. Moreover, the anisotropic potential suggests a noncentral Casimir force between two impurities. Our results would be beneficial for the study of impurity physics as well as the nontrivial effects brought about by SOC.

Up to now, we have only considered the single-phonon process and neglected the possible multiphonon process to obtain the instantaneous Casimir potential. This is valid for the weakly interacting two- and three-dimensional Bose gases at zero temperature (our case), where the fraction of the quantum depletion is rather small with a much smaller possibility of the multiphonon process. On the other hand, for 1D BEC at finite temperature, the quantum depletion becomes quite large, and the multiphonon process cannot be neglected. It has been pointed out that when the two-phonon exchanging process is included, the potential would become long ranged [48]. We leave the SOC effect on the Casimir potential with multiphonon process for future study.

Experimentally, BECs with Raman-induced 1D SOC have been realized in ultracold atom experiments [39,49–53] and many proposals on two-dimensional isotropic Rashba SOC have been made [54–56]. Moreover, techniques in detecting dynamics and correlations with single-atom resolution [57] have also been achieved. With these advances, our theoretical results may be verified in the near future.

ACKNOWLEDGMENTS

We acknowledge the helpful discussions with H. Pu and J. M. Zhang. This work was supported by the National Natural Science Foundation of China (NSFC) under Grants No. 61405003, No. 11404225, and No. 11474205 and Scientific Research Project of Beijing Educational Committee under Grants No. KM201510011002 and No. KM201510028005.

-
- [1] K. G. Wilson, *Rev. Mod. Phys.* **47**, 773 (1975).
 [2] P. Naidon and S. Endo, *Rep. Prog. Phys.* **80**, 056001 (2017).
 [3] H. Deng, H. Haug, and Y. Yamamoto, *Rev. Mod. Phys.* **82**, 1489 (2010).
 [4] B. N. Narozhny and A. Levchenko, *Rev. Mod. Phys.* **88**, 025003 (2016).
 [5] H. Alloul, J. Bobroff, M. Gabay, and P. J. Hirschfeld, *Rev. Mod. Phys.* **81**, 45 (2009).
 [6] E. Abrahams, S. V. Kravchenko, and M. P. Sarachik, *Rev. Mod. Phys.* **73**, 251 (2001).
 [7] P. A. Lee, N. Nagaosa, and X.-G. Wen, *Rev. Mod. Phys.* **78**, 17 (2006).
 [8] A. V. Balatsky, I. Vekhter, and J.-X. Zhu, *Rev. Mod. Phys.* **78**, 373 (2006).
 [9] F. Evers and A. D. Mirlin, *Rev. Mod. Phys.* **80**, 1355 (2008).
 [10] N. Nagaosa, Jairo Sinova, Shigeki Onoda, A. H. MacDonald, and N. P. Ong, *Rev. Mod. Phys.* **82**, 1539 (2010).
 [11] H. Hu, L. Jiang, H. Pu, Y. Chen, and X.-J. Liu, *Phys. Rev. Lett.* **110**, 020401 (2013).
 [12] L. Covaci and M. Berciu, *Phys. Rev. Lett.* **102**, 186403 (2009).
 [13] Y. E. Shchadilova, R. Schmidt, F. Grusdt, and E. Demler, *Phys. Rev. Lett.* **117**, 113002 (2016).
 [14] N. B. Jørgensen, L. Wacker, K. T. Skalmstang, M. M. Parish, J. Levinsen, R. S. Christensen, G. M. Bruun, and J. J. Arlt, *Phys. Rev. Lett.* **117**, 055302 (2016).
 [15] S. Shadkhoo and R. Bruinsma, *Phys. Rev. Lett.* **115**, 135305 (2015).
 [16] B. Casals, R. Cichelero, and P. G. Fernandez *et al.*, *Phys. Rev. Lett.* **117**, 026401 (2016).
 [17] M.-G. Hu, M. J. Van de Graaff, D. Kedar, J. P. Corson, E. A. Cornell, and D. S. Jin, *Phys. Rev. Lett.* **117**, 055301 (2016).
 [18] R. Schmidt and M. Lemeshko, *Phys. Rev. X* **6**, 011012 (2016).
 [19] J. D. Sau and E. Demler, *Phys. Rev. B* **88**, 205402 (2013).
 [20] L. A. Wray, S.-Y. Xu, Y. Xia, D. Hsieh, A. V. Fedorov, Y. S. Hor, R. J. Cava, A. Bansil, H. Lin, and M. Z. Hasan, *Nat. Phys.* **7**, 32 (2011).
 [21] A. H. Castro Neto, and F. Guinea, *Phys. Rev. Lett.* **103**, 026804 (2009).
 [22] P. W. Anderson, *Phys. Rev. Lett.* **18**, 1049 (1967).
 [23] M. Knap, A. Shashi, Y. Nishida, A. Imambekov, D. A. Abanin, and E. Demler, *Phys. Rev. X* **2**, 041020 (2012).
 [24] J. B. Balewski, A. T. Krupp, A. Gaj, D. Peter, H. P. Büchler, R. Löw, S. Hofferberth, and T. Pfau, *Nature* **502**, 664 (2013).
 [25] L. Yu, *Acta Phys. Sin.* **21**, 75 (1965).
 [26] H. Shiba, *Prog. Theor. Phys.* **40**, 435 (1968).
 [27] A. I. Rusinov, *Sov. Phys. JETP Lett.* **9**, 85 (1969).
 [28] S. Gopalakrishnan, C. V. Parker, and E. Demler, *Phys. Rev. Lett.* **114**, 045301 (2015).
 [29] P. M. R. Brydon, S. Das Sarma, H.-Y. Hui, and J. D. Sau, *Phys. Rev. B* **91**, 064505 (2015).
 [30] M. J. Bijlsma, B. A. Heringa, and H. T. C. Stoof, *Phys. Rev. A* **61**, 053601 (2000).
 [31] P. A. Martin and V. A. Zagrebnov, *Europhys. Lett.* **73**, 15 (2006).
 [32] X.-L. Yu, R. Qi, Z. B. Li, and W. M. Liu, *Europhys. Lett.* **85**, 10005 (2009).
 [33] Y. Nishida, *Phys. Rev. A* **79**, 013629 (2009).
 [34] M. Napiórkowski and J. Piasecki, *Phys. Rev. E* **84**, 061105 (2011).
 [35] J.-C. Jaskula, G. B. Partridge, M. Bonneau, R. Lopes, J. Ruaudel, D. Boiron, and C. I. Westbrook, *Phys. Rev. Lett.* **109**, 220401 (2012).
 [36] J. Marino, A. Recati, and I. Carusotto, *Phys. Rev. Lett.* **118**, 045301 (2017).
 [37] N. Goldman, G. Juzeliūnas, P. Öhberg, and I. B. Spielman, *Rep. Prog. Phys.* **77**, 126401 (2014).
 [38] H. Zhai, *Rep. Prog. Phys.* **78**, 026001 (2015).
 [39] Y.-J. Lin, K. Jiménez-García, and I. B. Spielman, *Nature* **471**, 83 (2011).
 [40] P.-S. He, Y.-H. Zhu, and W.-M. Liu, *Phys. Rev. A* **89**, 053615 (2014).
 [41] W. Yi and W. Zhang, *Phys. Rev. Lett.* **109**, 140402 (2012).
 [42] P. Fulde and R. A. Ferrell, *Phys. Rev.* **135**, A550 (1964); A. I. Larkin and Y. N. Ovchinnikov, *Sov. Phys. JETP* **20**, 762 (1965).
 [43] W. Zheng and Z. B. Li, *Phys. Rev. A* **85**, 053607 (2012).
 [44] C. Wang, C. Gao, C.-M. Jian, and H. Zhai, *Phys. Rev. Lett.* **105**, 160403 (2010).
 [45] M. A. Ruderman and C. Kittel, *Phys. Rev.* **96**, 99 (1954); T. Kasuya, *Prog. Theor. Phys. (Kyoto)* **16**, 45 (1956); K. Yosida, *Phys. Rev.* **106**, 893 (1957).
 [46] P.-S. He, R. Liao, and W.-M. Liu, *Phys. Rev. A* **86**, 043632 (2012).
 [47] G. D. Mahan, *Many-Particle Physics*, 3rd ed. (Plenum, New York, 2000), Sec. 5.4.
 [48] M. Schechter and A. Kamenev, *Phys. Rev. Lett.* **112**, 155301 (2014).
 [49] J.-Y. Zhang, S.-C. Ji, Z. Chen, L. Zhang, Z.-D. Du, B. Yan, G.-S. Pan, B. Zhao, Y.-J. Deng, H. Zhai, S. Chen, and J.-W. Pan, *Phys. Rev. Lett.* **109**, 115301 (2012).
 [50] P. J. Wang, Z.-Q. Yu, Z. K. Fu, J. Miao, L. H. Huang, S. J. Chai, H. Zhai, and J. Zhang, *Phys. Rev. Lett.* **109**, 095301 (2012).
 [51] L. W. Cheuk, A. T. Sommer, Z. Hadzibabic, T. Yefsah, W. S. Bakr, and M. W. Zwierlein, *Phys. Rev. Lett.* **109**, 095302 (2012).
 [52] C. Qu, C. Hamner, M. Gong, C. W. Zhang, and P. Engels, *Phys. Rev. A* **88**, 021604(R) (2013).

- [53] J. Li, W. Huang, B. Shteynas, S. Burchesky, F. C. Top, E. Su, J. Lee, A. O. Jamison, and W. Ketterle, *Phys. Rev. Lett.* **117**, 185301 (2016).
- [54] Q. Sun, L. Wen, W.-M. Liu, G. Juzeliūnas, and A.-C. Ji, *Phys. Rev. A* **91**, 033619 (2015).
- [55] S.-W. Su, S.-C. Gou, Q. Sun, L. Wen, W.-M. Liu, A.-C. Ji, J. Ruseckas, and G. Juzeliūnas, *Phys. Rev. A* **93**, 053630 (2016).
- [56] D. L. Campbell and I. B. Spielman, *New. J. Phys.* **18**, 033035 (2016).
- [57] H. Ott, *Rep. Prog. Phys.* **79**, 054401 (2016).